Preparation, structure, DNA-binding properties, and antioxidant activities of a homodinuclear erbium(III) complex with a pentadentate Schiff base ligand

Huilu Wu*, Guolong Pan, Yuchen Bai, Hua Wang, Jin Kong, Furong Shi, Yanhui Zhang and Xiaoli Wang

School of Chemical and Biological Engineering, Lanzhou Jiaotong University, Lanzhou 730070, P.R. China

An erbium (III) complex of a pentadentate Schiff base ligand [$(NO_3)Er(\mu\text{-}L)_2Er(NO_3)].2H_2O$ [H_2L=bis(*N*-salicylidene)-3-oxapentane-1,5-diamine] has been synthesised, characterised and its structure confirmed by X-ray crystallography. H_2L and the Er(III) complex both bind to DNA *via* a groove binding mode, and the Er(III) complex binds to DNA more strongly than H_2L. The complex shows strong scavenging effects for hydroxyl radicals (OH·) and superoxide radicals ($O_2^{-\cdot}$).

Keywords: Schiff base, erbium(III) complex, crystal structure, DNA-binding, antioxidant activity

Many chemicals exert antitumour effects through binding to DNA, thereby changing the replication of DNA and inhibiting the growth of the tumour cells. This is the basis of designing new and more efficient antitumour drugs, and their effectiveness depends on the mode and affinity of the binding.[1,2] A number of metal chelates, as agents for mediation of strand scission of duplex DNA and as chemotherapeutic agents, have been used as probes of DNA structure in solution.[3–5] The biological activities shown by DNA-binder metal complexes are various and are often related to their specific DNA-binding mechanism, ranging from intercalation to covalent and groove binding.[6,7] Therefore, an understanding of how these small molecules bind to DNA will potentially be useful in the design of new compounds that can recognise specific sites or conformations of DNA.[8–10]

Their biological activity and a number of other applications have resulted in strongly increasing interest in lanthanide compounds in the last decade.[11–14] One of the most studied applications is the use of lanthanide complexes to address DNA/RNA interaction by non-covalent binding and/or cleavage.[15–17] Moreover, interest in the chelation of metal ions by Schiff base macrocyclic (coronand) and open-chain (podand) ligands has continually increased owing to the recognition of the role played by these structures in bioinorganic and medicinal inorganic chemistry.[18,19] We now present the synthesis, characterisation and DNA-binding properties of an erbium(III) complex with a pentadentate Schiff base ligand, bis(*N*-salicylidene)-3-oxapentane-1,5-diamine. In addition, the antioxidant properties of the Er(III) complex are discussed in detail.

Experimental

C, H, and N elemental analyses were determined using a Carlo Erba 1106 elemental analyser. IR spectra were recorded from 4000–400 cm^{-1} with a Nicolet FT-VERTEX 70 spectrometer using KBr pellets. Electronic spectra were taken on Lab-Tech UV Bluestar and Spectrumlab 722sp spectrophotometers (0.2 nm spectral resolution). Fluorescence spectra were recorded on a LS-45 spectrofluorophotometer. ^{1}H NMR spectra were obtained with a Mercury plus 400 MHz NMR spectrometer with TMS as internal standard and $CDCl_3$ as solvent.

All chemicals were of analytical grade. Calf thymus DNA (CT-DNA), ethidium bromide (EB), nitroblue tetrazolium nitrate (NBT), methionine (MET) and riboflavin ($VitB_2$) were obtained from Sigma-Aldrich Co. (USA) and used without purification. All experiments involving interaction of the ligand and the complex with CT-DNA were carried out in a doubly-distilled water buffer containing 5 mM Tris and 50 mM NaCl adjusted to pH = 7.2 with hydrochloric acid. A solution of CT-DNA gave a ratio of UV absorbance at 260 and 280 nm of about 1.8–1.9, indicating that the CT-DNA was sufficiently free of protein.[20] The CT-DNA concentration per nucleotide was determined spectrophotometrically by employing an extinction coefficient of 6600 $M^{-1}\cdot cm^{-1}$ at 260 nm.[21]

The synthetic route for the ligand precursor H_2L is shown in Scheme 1.

3-Oxapentane-1,5-diamine: Synthesised following the procedure in ref. 22. Anal. calcd for $C_4H_{12}N_2O$: C, 46.3; H, 11.5; N, 26.9; found: C, 46.0; H, 11.5; N, 26.8%. FT–IR (KBr ν/cm^{-1}): 1120, ν(C–O–C); 3340, ν(–NH_2).

bis(N-Salicylidene)-3-oxapentane-1,5-diamine (H_2L): Salicylic aldehyde (10 mmol, 1.22 g) in EtOH (5 mL) was added dropwise to an EtOH solution (5 mL) of 3-oxapentane-1,5-diamine (5 mmol, 0.52 g). After the completion of addition, the solution was stirred for an additional 4 h at 78 °C. After cooling to room temperature, the precipitate was filtered. The product was dried *in vacuo*, to give a yellow crystalline solid. Yield: 1.2 g (68.5%). Anal. calcd for $C_{18}H_{20}O_3N_2$: C, 69.2; H, 6.4; N, 9.0; found: C, 69.1; H, 6.5; N, 8.8%. ^{1}H NMR ($CDCl_3$ 400 MHz) δ/ppm: 8.30 (s, 2H, N=C–H), 6.79–7.33 (m, 8H, H-benzene ring), 3.66–3.74 (m, 8H, O–$(CH_2)_2$–N=C). UV-Vis (λ, nm): 268, 316. FT–IR (KBr ν/cm^{-1}): 1637, ν(C=N); 1286, ν(C–O–C); 3458, ν(OH).

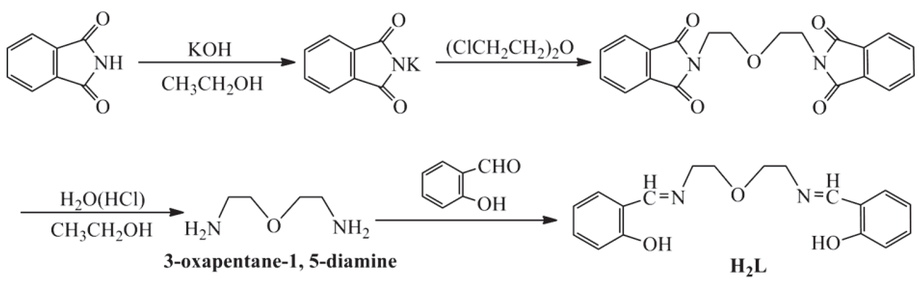

Scheme 1 Synthesis of ligand H_2L.

* Correspondent. E-mail: wuhuilu@163.com

Complex [$(NO_3)Er(\mu\text{-}L)_2Er(NO_3)$].2$H_2O$ (**1**): To a stirred solution of H_2L (156 mg, 0.5 mmol) in EtOH (10 mL) was added $Er(NO_3)_3(H_2O)_6$ (231 mg 0.5 mmol) and triethylamine (0.3 mL) in EtOH (10 mL). A yellow sediment was generated rapidly. The precipitate was filtered off, washed with EtOH and absolute Et_2O, and dried in *vacuo*. The dried precipitate was dissolved in DMF to form a yellow solution. Yellow block crystals of **1**, suitable for X-ray diffraction studies, were obtained by vapour diffusion of diethyl ether into the solution for a few weeks at room temperature. Yield: 207 mg (53.5%). Anal. calcd for $C_{36}H_{40}Er_2N_6O_{14}$: C, 38.8; H, 3.6; N, 7.5; found: C, 38.6; H, 3.8; N, 7.4%. UV-Vis (λ, nm): 269, 316. FT–IR (KBr ν/cm^{-1}): 1276, ν(C–O–C); 1382, $\nu_s(NO_3)$; 1055, $\nu_a(NO_3)$; 1634 ν(C=N).

X-ray crystallography

A suitable single crystal of **1** was mounted on a glass fibre, and the intensity data were collected on a Bruker Smart CCD diffractometer with graphite-monochromated Mo-Kα radiation (λ = 0.71073 Å) at 296 K. Data reduction and cell refinement were performed using the SMART and SAINT programs.[23] The structure was solved by direct methods and refined by full-matrix least-squares against F^2 of data using SHELXTL software.[24] All H atoms were found in difference electron maps and subsequently refined in a riding-model approximation with C–H distances ranging from 0.93 to 0.97 Å and U_{iso} (H) = 1.2 U_{eq}(C) or 1.5 U_{eq}(C). The crystal data and experimental parameters relevant to the structure determination are listed in Table 1. Selected bond lengths and angles are presented in Table 2.

DNA-binding experiments

Viscosity experiments were conducted on an Ubbelodhe viscometer, immersed in a water bath maintained at 25.0 ± 0.1 °C. Titrations were performed for compounds (3–30 μM), and each compound was introduced into a CT-DNA solution (42.5 μM) present in the viscometer. Data were analysed as $(\eta/\eta_0)^{1/3}$ *versus* the ratio of the concentration of the compound to CT-DNA, where η is the viscosity of CT-DNA in the presence of the compound and η_0 is the viscosity of CT-DNA alone. Viscosity values were calculated from the observed flow time of CT-DNA-containing solutions corrected from the flow time of buffer alone (t_0), $\eta = (t - t_0)$.[25]

Table 1 Crystal/structure refinement data for [$(NO_3)Er(\mu\text{-}L)_2Er(NO_3)$].2$H_2O$ (**1**)

Complex	**1**
Molecular formula	$C_{36}H_{40}Er_2N_6O_{14}$
Molecular weight	1115.26
Colour, habit	Yellow, block
Crystal size/mm^3	0.26 × 0.23 × 0.21
Crystal system	Monoclinic
Space group	*C*2/*c*
a/Å	29.35(2)
b/Å	11.748(9)
c/Å	15.231(12)
β/deg	118.235(6)
V/Å^3	4627(6)
Z	4
Absorption coefficient/mm^{-1}	3.666
T/K	296(2)
D_{calcd}/g cm^{-3}	1.601
F (000)/e	2184
θ range for data collection, deg	2.19 to 25.50
hkl range	–35, 35/ –11, 14/ –18, 17
Reflections collected	11947
Independent reflections/R_{int}	4265/0.0298
Data/restraints/parameters	4265/3/262
Final R_1/wR_2 indices [$I > 2\sigma(I)$]	0.0296/0.0756
R_1/wR_2 indices (all data)[a]	0.0459/0.0836
Goodness-of-fit on F^2	1.111
Largest diff. peak/hole/e Å^{-3}	0.882/–0.872

Absorption titration experiments were performed with fixed concentrations of a compound, while gradually increasing the concentration of CT-DNA. To obtain the absorption spectra, the required amount of CT-DNA was added to both the compound and reference solutions, in order to eliminate the absorbance of CT-DNA itself. From the absorption titration data, the binding constant (K_b) was determined using the equation:[26]

$$[DNA]/(\varepsilon_a - \varepsilon_f) = [DNA]/(\varepsilon_b - \varepsilon_f) + 1/K_b(\varepsilon_b - \varepsilon_f)$$

where [DNA] is the concentration of CT-DNA in base pairs, ε_a corresponds to the observed extinction coefficient (Aobsd/[M]), ε_f corresponds to the extinction coefficient of the free compound, ε_b is the extinction coefficient of the compound when fully bound to CT-DNA, and K_b is the intrinsic binding constant. The ratio of slope to intercept in the plot of $[DNA]/(\varepsilon_a - \varepsilon_f)$ *versus* [DNA] gave the value of K_b.

The enhanced fluorescence of EB in the presence of DNA can be quenched by the addition of a second molecule.[16,27] The extent of fluorescence quenching of EB bound to CT-DNA can be used to determine the extent of binding between the second molecule and CT-DNA. Competitive binding experiments were carried out in the buffer by keeping [DNA]/[EB] = 1 and varying the concentrations of the compounds. The fluorescence spectra of EB were measured using an excitation wavelength of 520 nm, and the emission range was set between 550 and 750 nm. The spectra were analysed according to the classical Stern–Volmer equation:[28]

$$I_0/I = 1 + K_{SV}[Q]$$

where I_0 and I are the fluorescence intensities at 599 nm in the absence and presence of the quencher, respectively, K_{SV} is the linear Stern–Volmer quenching constant, and [Q] is the concentration of the quencher. In these experiments, [CT-DNA] = 2.5 × 10^{-3} mol L^{-1}, [EB] = 2.2 × 10^{-3} mol L^{-1}.

Antioxidation study methods

Hydroxyl radicals were generated in aqueous media by a Fenton-type reaction.[29] The aliquots of reaction mixture (3 mL) contained 1 mL of 0.1 mmol aqueous safranin, 1 mL of 1.0 mmol aqueous EDTA–Fe(II), 1 mL of 3% aqueous H_2O_2, and a series of quantitative microadditions of solutions of the test compound. A sample without the tested compound was used as the control. The reaction mixtures were incubated at 37 °C for 30 min in a water bath. The absorbance was then measured at 520 nm. All the tests were run in triplicate and are

Table 2 Selected bond lengths (Å) and bond angles (deg) for **1**

Bond lengths			
Er(1)–O(3)	2.161(4)	Er(1)–O(2)#1[a]	2.271(4)
Er(1)–O(2)	2.306(4)	Er(1)–O(5)	2.446(4)
Er(1)–O(1)	2.449(4)	Er(1)–O(4)	2.469(4)
Er(1)–N(2)	2.473(5)	Er(1)–N(1)	2.496(5)
Bond angles			
O(3)–Er(1)–O(2)#1	96.45(15)	O(3)–Er(1)–O(2)	85.09(14)
O(2)#1–Er(1)–O(2)	71.11(15)	O(3)–Er(1)–O(5)	95.94(17)
O(2)#1–Er(1)–O(5)	156.99(13)	O(2)–Er(1)–O(5)	129.34(14)
O(3)–Er(1)–O(1)	140.89(15)	O(2)#1–Er(1)–O(1)	87.13(14)
O(2)–Er(1)–O(1)	132.05(14)	O(5)–Er(1)–O(1)	71.12(15)
O(3)–Er(1)–O(4)	81.96(16)	O(2)#1–Er(1)–O(4)	149.82(13)
O(2)–Er(1)–O(4)	78.74(13)	O(5)–Er(1)–O(4)	51.60(14)
O(1)–Er(1)–O(4)	113.08(15)	O(3)–Er(1)–N(2)	74.94(18)
O(2)#1–Er(1)–N(2)	85.08(15)	O(2)–Er(1)–N(2)	146.97(16)
O(5)–Er(1)–N(2)	79.52(16)	O(1)–Er(1)–N(2)	66.55(18)
O(4)–Er(1)–N(2)	122.86(15)	O(3)–Er(1)–N(1)	151.51(16)
O(2)#1–Er(1)–N(1)	90.01(15)	O(2)–Er(1)–N(1)	70.80(14)
O(5)–Er(1)–N(1)	88.28(17)	O(1)–Er(1)–N(1)	66.93(15)
O(4)–Er(1)–N(1)	78.71(16)	N(2)–Er(1)–N(1)	133.40(17)

[a]Symmetry transformations used to generate equivalent atoms: #1 – *x* + 1/2, –*y* + 1/2, –*z*.

expressed as the mean and standard deviation (SD).[27,29] The scavenging effect for OH· was calculated from the following expression:

$$\text{Scavenging ratio (\%)} = [(A_i - A_0)/(A_c - A_0)] \times 100\%$$

where A_i = absorbance in the presence of the test compound; A_0 = absorbance of the blank; A_c = absorbance in the absence of the test compound, EDTA-Fe(II) and H_2O_2.

A nonenzymatic system containing 1 mL 9.9×10^{-6} M VitB2, 1 mL 1.38×10^{-4} M NBT, 1 mL 0.03 M MET was used to produce superoxide anion (O_2^{-}), and the scavenging rate of O_2^{-} under the influence of 0.1–1.0 μM of the tested compound was determined by monitoring the reduction in rate of transformation of NBT to monoformazan dye.[30] The solutions of MET, VitB2 and NBT were prepared with 0.02 M phosphate buffer (pH = 7.8) at the condition of avoiding light. The reactions were monitored at 560 nm with a UV-Vis spectrophotometer, and the rate of absorption change was determined. The percentage inhibition of NBT reduction was calculated using the following equation:[31]

$$\text{Percentage inhibition of NBT reduction} = (1 - k'/k) \times 100$$

where k' and k represent the slopes of the straight line of absorbance values as a function of time in the presence and absence of SOD mimic compound (SOD is superoxide dismutase), respectively. The IC_{50} values for the complexes were determined by plotting the graph of percentage inhibition of NBT reduction against the increase in the concentration of the complex. The concentration of the complex which causes 50% inhibition of NBT reduction is reported as IC_{50}.

Results and discussion

The Er(III) complex **1** was prepared by reaction of H_2L with $Er(NO_3)_3(H_2O)_6$ in ethanol. It is soluble in polar aprotic solvents such as DMF, DMSO and MeCN, slightly soluble in ethanol, methanol, ethyl acetate, and chloroform and insoluble in water, Et_2O and petroleum ether. The elemental analysis shows that its composition is $Er_2(L)_2(NO_3)_2 \cdot 2H_2O$ and its was confirmed by the crystal structure analysis.

For the free ligand H_2L, a strong band is found at 1637 cm^{-1} together with a weak band at 1286 cm^{-1}. By analogy with previously assigned bands, the former can be attributed to ν(C=N), while the latter can be attributed to ν(C–O–C). These bands were shifted to lower frequency by *ca* 3–10 cm^{-1} for **1**,[32] which implies direct coordination of the nitrogen and oxygen atoms to metal ions. Bands at 1382 and 1055 cm^{-1} indicate that nitrate is bidentate[33] and a weak band at 3663 cm^{-1} is allocated as $\nu(H_2O)$, in agreement with the result of X-ray diffraction.

The electronic spectra of the ligand H_2L and **1** were recorded in DMF solution at room temperature. The UV bands of H_2L (268, 316 nm) are marginally shifted in the complex. That two absorption bands are assigned to $\pi \rightarrow \pi^*$(benzene) and $\pi \rightarrow \pi^*$ (C=N) transitions.[34]

X-ray structure of the complex

The crystal structure of **1** consists of discrete $[(NO_3)Er(\mu\text{-}L)_2Er(NO_3)]$ units and two H_2O solvent molecules. The prepared pentadentate ligand contains strong donors, namely phenoxo-oxygen atoms as well as imine nitrogen atoms, with excellent coordination ability for transition/inner-transition metal ions through its N_2O_3 donor set. Single crystal X-ray structure determination revealed that the complex has a centrosymmetric neutral homodinuclear entity. An ORTEP illustration of the complex (Fig. 1a) shows that two adjacent $[Er(L)(NO_3)]$ moieties are bridged *via* two phenoxo groups. In the μ_2-diphenoxo bridged binuclear structure, both Er(III) centres are octacoordinated. The local coordination environment is identical for both centres by symmetry and is best described as a distorted square ErN_2O_6 antiprism (Fig. 1b). Due to the flexibility of the ligand, it loses planarity. The nature of coordination of the two identical Schiff base moieties of the same ligand is completely different and hence noteworthy. Of the two phenoxo oxygen atoms coming out of each ligand, one is simply monocoordinated while the other one bridges the adjacent Er(III) centres as reflected by the Er–$O_{phenoxo}$ bond lengths [Er(1)–O(2), 2.306(4) and Er(1)–O(2A), 2.271(4) Å]. The distance of Er(1)–Er(1A): 3.724(3) Å is relatively too long to consider any direct intramolecular Er–

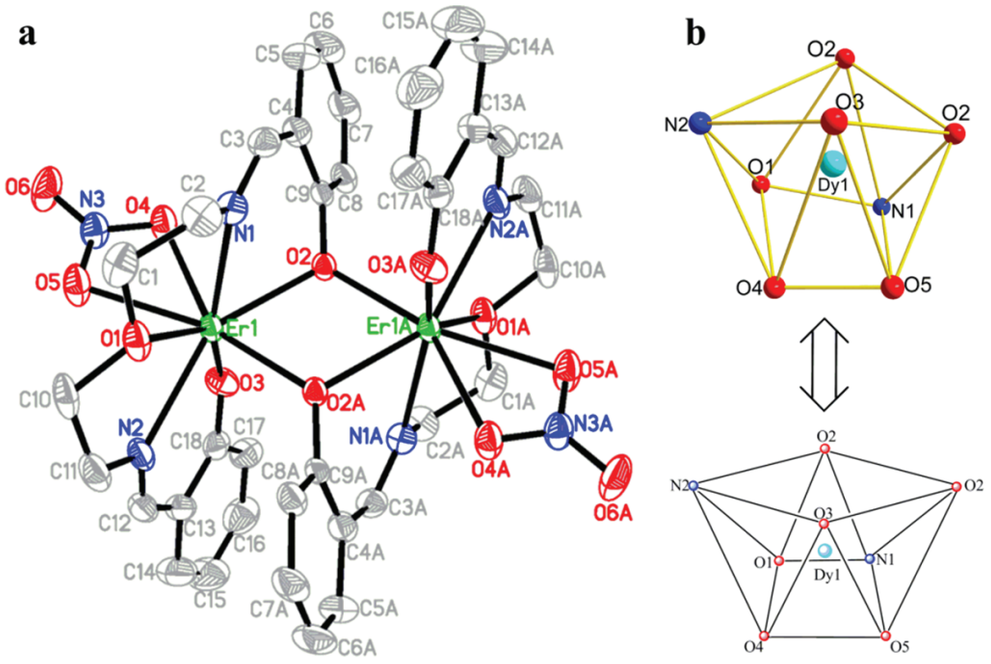

Fig. 1 (a) The molecular structure of $Er_2L_2(NO_3)_2$ in the crystal with displacement ellipsoids at the 30% probability level; H atoms are omitted for clarity, (b) A distorted square antiprism geometry is formed by donor atoms around the Er^{3+} centre as illustrated in the polyhedral view.

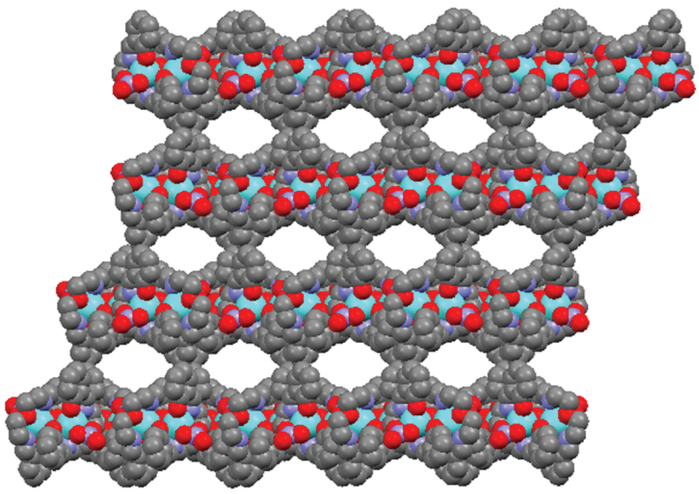

Fig. 2 A space-filling diagram of the nanosized holes in the Er(III) complex. In order to simplify, water solvent molecules are omitted for clarity.

Er interaction. Hydrogen-bonding interactions play important roles in crystal packing in the complex. An interesting feature of this structure is the intermolecular hydrogen bond that exists among the Er(III) complexes, which also affords voids to trap guest molecules (Fig. 2). Note that intermolecular interactions have the potential to assemble smaller and simpler fragments into desired cavities under favourable conditions, which is important in host–guest chemistry and has applications in chemistry, biology and materials science.

DNA-binding properties

Viscosity measurements

Viscosity titration measurements were carried out to further clarify the interaction modes between the investigated compounds and CT-DNA. Hydrodynamic measurements that are sensitive to changes in the length of DNA (*i.e.* viscosity and sedimentation) are regarded as the least ambiguous and the most critical tests of binding in solution in the absence of crystallographic structural data.[27] The classic intercalation model involves the insertion of a planar molecule between DNA base pairs, which results in a decrease in the DNA helical twist and lengthening of the DNA, the molecule will also be in close proximity to the DNA base pairs.[29] In contrast, molecules that bind exclusively in the DNA grooves by partial and/or non-classical intercalation, under the same conditions, typically cause less pronounced (positive or negative) or no change in DNA solution viscosity.[35]

The effects of H_2L and **1** on the viscosity of CT-DNA are shown in Fig. 3. The experimental results show that the addition of H_2L and **1** causes no significant viscosity change. Therefore, according to a previous report relating to DNA-binding lanthanide complexes,[16,35] we can deduce that H_2L and **1** most probably bind to DNA in a groove mode. The reason for the DNA–binding modes for the ligand and **1** can be attributed to steric hindrance and electron density, which are both caused by the geometric structure.

Electronic absorption spectroscopy

The application of electronic absorption spectroscopy is one of the most useful techniques in DNA-binding studies.[17] To clarify the interactions between the compounds and DNA, the electronic absorption spectra of the ligand H_2L and its **1** in the absence and in the presence of the CT-DNA (at a constant concentration of the compounds) were obtained and are shown in Fig. 4. With increasing DNA concentrations, the absorption bands at 394 nm of H_2L show a hypochromism of 32.5%; the absorption bands at 392 nm of **1** show a hypochromism of 63.8%. The hypochromism observed for the $\pi \rightarrow \pi^*$ transition bands indicating strong binding of H_2L and complex to DNA.

To compare quantitatively the affinity of H_2L and **1** towards DNA, the intrinsic binding constants K_b of the two compounds

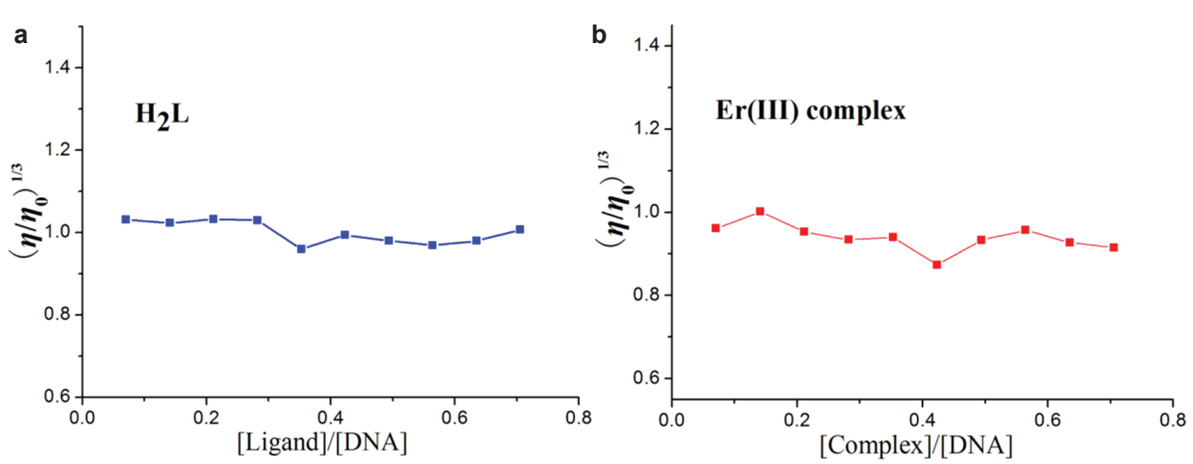

Fig. 3 Effect of increasing amounts of H_2L(a) and **1**(b) on the relative viscosity of CT-DNA at 25.0 ± 0.1 °C.

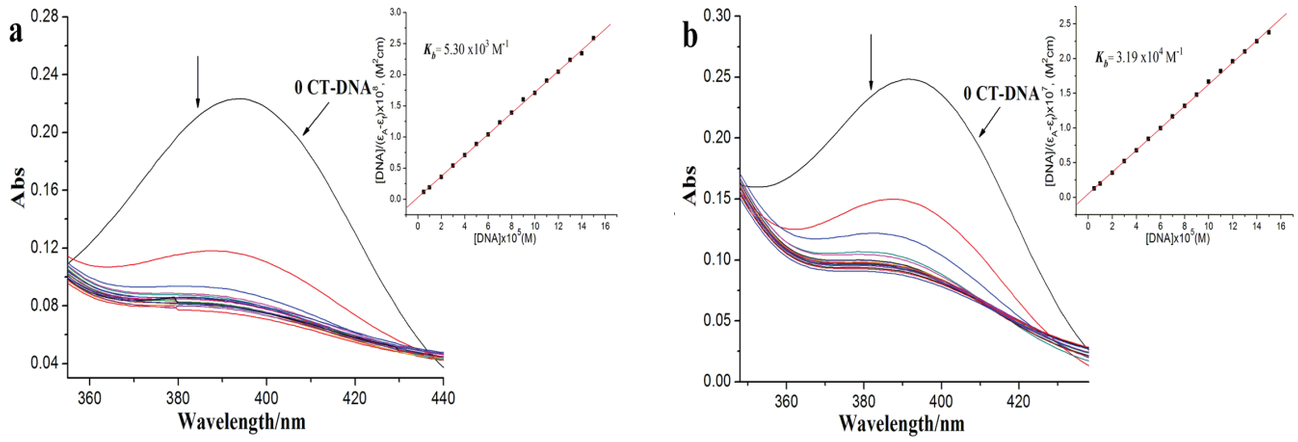

Fig. 4 Absorption spectra of compound in the presence of CT-DNA (the DNA absorption was subtracted). The concentration of H_2L (a) and **1**(b), was kept constant at 3×10^{-5} M^{-1}. Arrows show the absorbance changes upon increasing DNA concentration. Inset: Plots of [DNA]/($\varepsilon_a-\varepsilon_f$) *versus* [DNA] for the titration of DNA with compound; ■, experimental data points; solid line, linear fitting of the data.

to CT-DNA were determined by monitoring the changes of absorbance with increasing concentration of DNA. The intrinsic binding constant K_b of H_2L and of **1** were $(5.30\pm0.096)\times10^3$ M^{-1} (R = 0.99 for 16 points) and $(3.19\pm0.104)\times10^4$ M^{-1} (R = 0.99 for 16 points), respectively, from the decay of the absorbances. The K_b values obtained here are lower than that reported for a classical intercalator (for ethidium bromide and [Ru(phen) DPPZ], binding constants are of the order of 10^6–10^7 M^{-1}).[36,37] It is clear that the hypochromism and K_b values can suggest an intimate association of the compounds with CT-DNA and indicate that the binding strength of **1** is higher than for H_2L.

Based on the above results, the affinity for DNA is stronger for **1** than H_2L. We consider that the most likely reason is that the charge transfer of coordinated H_2L, caused by coordination of the central atom, results in the decrease of charge density of the planar conjugated system. This change will lead to complexes binding to DNA more easily.[27,29] Moreover, the helix structure of the Er(III) complex is able to provide lots of grooving positions to stack more strongly with the base pairs of the DNA helix.[16]

Fluorescence spectra

In order to further study the binding properties of the complexes with DNA, competitive binding experiments were carried out. Relative binding of H_2L and **1** to CT-DNA was studied by the fluorescence spectral method using ethidium bromide (EB) bound CT-DNA solution in Tris-HCl/NaCl buffer (pH = 7.2). As a typical indicator of intercalation, EB is a weakly fluorescent compound, but in the presence of DNA, its emission intensity is greatly enhanced because of its strong intercalation between the adjacent DNA base pairs.[38] In general, measurement of the ability of a complex to affect the intensity of EB fluorescence in the EB-DNA adduct allows determination of the affinity of the complex for DNA. If a complex can displace EB from DNA, the fluorescence of the solution will be reduced due to the fact that free EB molecules are readily quenched by the solvent water.[39] For ligand H_2L and **1**, no emission was observed neither alone nor in the presence of CT-DNA in the buffer. The fluorescence quenching of DNA–bound EB by the ligand and complex are shown in Fig. 5. The behaviour of H_2L and **1** are in good agreement with the Stern–Volmer equation, which provides further evidence that the two compounds bind to DNA. The K_{sv} values for H_2L and **1** are $(0.35\pm0.010)\times10^4$ (R = 0.98 for 21 points in the line part) and $(2.51\pm0.083)\times10^4$ M^{-1} (R = 0.98 for 13 points), respectively, reflecting the higher quenching efficiency of **1** relative to that of H_2L. This result suggests that the DNA-binding of **1** is stronger than that of H_2L. Such a trend is consistent with the previous absorption spectral results.

Antioxidant activities

According to relevant reports in the literature,[40,41] the rare earth complexes may exhibit antioxidant activity. We therefore also conducted an investigation to explore whether **1** has antioxidant activities.

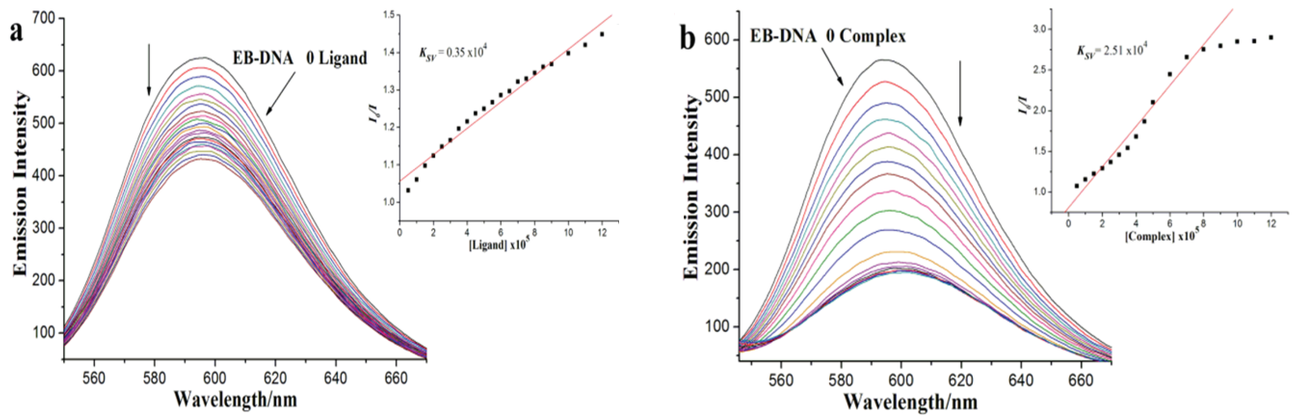

Fig. 5 Fluorescence spectra of the DMF solution of H_2L (a) and **1** (b) in Tris–HCl buffer upon addition of CT-DNA. [Compound] = 3×10^{-5} M^{-1}. Arrows show the intensity changing upon increasing CT-DNA concentrations. Sterne–Volmer quenching plots of the ligand and **1** are inset in their own fluorescence spectra with increasing concentrations of CT-DNA.

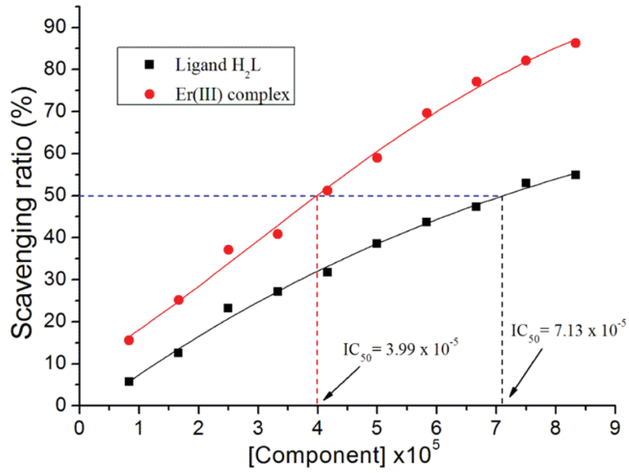

Fig. 6 The inhibitory effect of the ligand and **1** on OH· radicals; the suppression ratio increases with increasing concentration of the test compound.

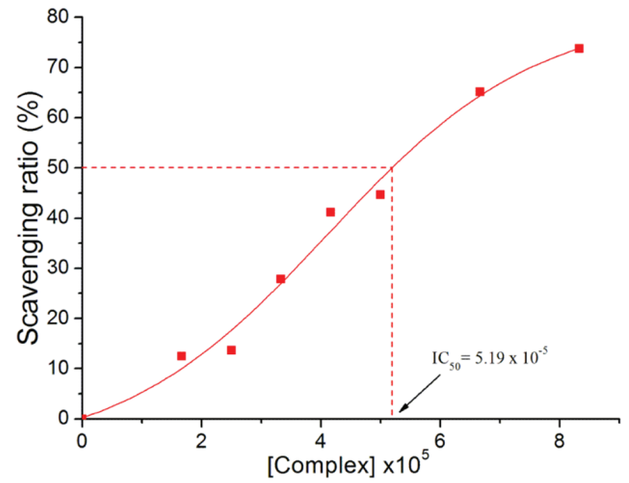

Fig. 7 The inhibitory effect of **1** on $O_2^{\cdot-}$ radicals; the suppression ratio increases with increasing concentration of the test compound.

Hydroxyl radical scavenging activity: Figure 6 shows the plots of hydroxyl radical scavenging effects (%) for the ligand and **1**. The values of IC_{50} of the ligand and **1** for hydroxyl radical scavenging effects are $(7.13 \pm 0.097) \times 10^{-5}$ M and $(3.99 \pm 0.070) \times 10^{-5}$ M, respectively. It is thus proved that the hydroxyl radical scavenging effect of **1** is much higher than that of the ligand. Moreover, we compared the abilities of the present compounds to scavenge hydroxyl radical (OH·) with those of the well-known natural antioxidants mannitol and vitamin C, using the same method as reported in a previous paper.[42] The 50% inhibitory concentration (IC_{50}) value of mannitol and vitamin C are about 9.6×10^{-3} and 8.7×10^{-3} M, respectively. The results imply that **1** has a greater ability to scavenge hydroxyl radical (OH·) than mannitol and vitamin C. It can be concluded that a much less or no scavenging activity was exhibited by the ligand when compared to that of its complex, which is due to the chelation of ligand with the central metal atom.[42] The observed IC_{50} values for **1** suggest that it could be considered as a potential drug to eliminate the hydroxyl radical.

Superoxide radical scavenging activity: As another assay of antioxidant activity, superoxide radical ($O_2^{\cdot-}$) scavenging activity has been investigated. Complex **1** has good superoxide radical scavenging activity. The Er(III) complex shows an IC_{50} value of $(5.19 \pm 0.089) \times 10^{-5}$ M (Fig. 7), which indicates that it has potent scavenging activity for superoxide radical ($O_2^{\cdot-}$). This indicates that **1** might be an inhibitor (or a drug) to scavenge $O_2^{\cdot-}$ *in vivo,* which merits further investigation.

Conclusions

In this work, a pentadentate Schiff base ligand bis(*N*-salicylidene)-3-oxapentane-1,5-diamine and its Er(III) complex have been synthesised and characterised. The binding modes of these compounds with CT-DNA have been studied by electronic absorption titration, ethidium bromide–DNA displacement experiments and viscosity measurements. The results indicate that the ligand H_2L and complex **1** bind to DNA in a groove mode, and the affinity for DNA is stronger for **1** when compared with the ligand. In addition, **1** also has active scavenging effects on the OH· and $O_2^{\cdot-}$ radicals. Our research should be valuable for seeking and designing new antitumour drugs and antioxidants, as well as for understanding the mechanism of DNA-binding.

Crystallographic data (excluding structure factors) for the structure in this paper have been deposited with the Cambridge Crystallographic Data Centre, CCDC, 12 Union Road, Cambridge CB2 1EZ, UK. Copies of the data can be obtained free of charge on quoting the depository number CCDC-936140 (Fax: +44 1223 336033; E-mail: deposit@ccdc.cam.ac.uk, http://www.ccdc.cam.ac.uk).

The present research was supported by the National Natural Science Foundation of China (Grant No. 21367017), the Fundamental Research Funds for the Gansu Province Universities (212086), National Natural Science Foundation of Gansu Province (Grant No. 1212RJZA037), and 'Qing Lan' Talent Engineering Funds for Lanzhou Jiaotong University.

Received 21 January 2014; accepted 7 February 2014
Paper 1402418 doi: 10.3184/174751914X13933417974082
Published online:2 April 2014

References

1 Y.B. Zeng, N. Yang, W.S. Liu and N. Tang, *J. Inorg. Biochem.*, 2003, **97**, 258.
2 V. Rajendiran, R. Karthik, M. Palaniandavar, H. Stoeckli-Evans, V.S. Periasamy, M.A. Akbarsha, B.S. Srinag and H. Krishnamurthy, *Inorg. Chem.*, 2007, **46**, 8208.
3 M. Demeunynck, C. Bailly and W.D. Wilson (eds.) *Small molecule DNA and RNA binders:from synthesis to nucleic acid complexes*. Wiley-VCH, Weinheim (2003).
4 R.W.Y. Sun, D.L. Ma, E.L.M. Wong and C.M. Che, *J. Chem. Soc. Dalton Trans*, 2007, **2007**, 4884.
5 C. Moucheron, *New J. Chem.*, 2009, **33**, 235.
6 M.J. Hannon, *Chem. Soc. Rev.*, 2007, **36**, 280.
7 G.L. Pan, Y.C. Bai, H. Wang, J. Kong, F.R. Shi, Y.H. Zhang, X.L. Wang and H.L. Wu, *Z. Naturforsch. B*, 2013, **68**, 257.
8 K.E. Erkkila, D.T. Odom and J.K. Barton, *Chem. Rev.*, 1999, **99**, 2777.
9 L.N. Ji, X.H. Zou and J.G. Liu, *Coord. Chem. Rev.*, 2001, **216–217**, 513.
10 B.M. Zeglis, V.C. Pierre and J.K. Barton, *Chem. Commun.*, 2007, **44**, 4565.
11 F.H. Lia, G.H. Zhao, H.X. Wu, H. Lin, X.X. Wu, S.R. Zhu and H.K. Lin, *J. Inorg. Biochem.*, 2006, **100**, 36.
12 H.X. Xu, H.Y. Zhang and X.G. Qu, *J. Inorg. Biochem.*, 2006, **100**, 1646.
13 A. Cha, G.E. Snyder, P.R. Selvin and F. Bezanilla, *Nature*, 1999, **402**, 809.
14 P. Caravan, J. Ellison, T. McMurry and R. Lauffer, *Chem. Rev.*, 1999, **99**, 2293.
15 M. Marinić, I. Piantanida, G. Rusak and M. Žinić, *J. Inorg. Biochem.*, 2006, **100**, 288.
16 Z.Y. Yang, B.D. Wang and Y.H. Li, *J. Organometal. Chem.*, 2006, **691**, 4156.
17 P. Kapoor, R.V. Singh and N. Fahmi, *J. Coord. Chem.*, 2012, **65**, 262.
18 W. Radecka-Paryzek, V. Patroniak and J. Lisowski, *Coord. Chem. Rev.*, 2005, **249**, 2156.

19 P.A. Vigato and S. Tamburini, *Coord. Chem. Rev.*, 2004, **248**, 1717.
20 S. Satyanaryana, J.C. Dabrowiak and J.B. Chaires, *Biochemistry*, 1993, **32**, 2573.
21 J. Marmur, *J. Mol. Biol.*, 1961, **3**, 208.
22 S.M. Nalson and V. Knox, *J. Chem. Soc. Dalton Trans.*, 1983, **1983**, 2525.
23 Bruker, *Smart saint and sadabs*. Bruker Axs, Inc, Madison, WI, 2000.
24 G.M. Sheldrick, SHELXTL, Siemens Analytical X-ray Instruments, Inc., Madison, Wisconsin, 1996.
25 C.P. Tan, J. Liu, L.M. Chen, S. Shi and L.N. Ji, *J. Inorg. Biochem.*, 2008, **102**, 1644.
26 A.M. Pyle, J.P. Rehmann, R. Meshoyrer, C.V. Kumar, N.J. Turro and J.K. Barton, *J. Am. Chem. Soc.*, 1989, **111**, 3051.
27 H.L. Wu, J.K. Yuan, Y. Bai, G.L. Pan, H. Wang, J. Kong, X.Y. Fan and H.M. Liu, *J. Chem. Soc. Dalton Trans.*, 2012, **2012**, 8829.
28 J.R. Lakowicz and G. Webber, *Biochemistry*, 1973, **12**, 4161.
29 H.L. Wu, J.K. Yuan, Y. Bai, G.L. Pan, H. Wang and X.B. Shu, *J. Photochem. Photobiol. B*, 2012, **107**, 65.
30 C. Beauchamp and I. Fridovich, *Anal. Biochem.*, 1971, **44**, 276.
31 Q.H. Luo, Q. Lu, A.B. Dai and L.G. Huang, *J. Inorg. Biochem.*, 1993, **51**, 655.
32 W.K. Dong, G. Wang, S.S. Gong, J.F. Tong, Y.X. Sun and X.H. Gao, *Transit. Metal Chem.*, 2012, **37**, 271.
33 K. Nakamoto, *Infrared and Raman spectra of inorganic and coordination compounds*, 4th edn. John Wiley & Sons, New York, 1986, p. 284.
34 L. Casella, M. Gullotti, A. Pintar, L. Messori, A. Rockenbauer and M. Györ, *Inorg. Chem.*, 1987, **26**, 1031.
35 B.D. Wang, Z.Y. Yang, P. Crewdson and D.Q. Wang, *J. Inorg. Biochem.*, 2007, **101**, 1492.
36 V.G. Vaidyanathan and B.U. Nair, *J. Inorg. Biochem.*, 2003, **94**, 121.
37 R. Vijayalakshmi, M. Kanthimathi, V. Subramanian and B.U. Nair, *Biochim. Biophys. Acta*, 2000, **1475**, 157.
38 H.L. Wu, J.K. Yuan, Y. Bai, H. Wang, G.L. Pan and J. Kong, *J. Photochem. Photobiol. B*, 2012, **116**, 13.
39 J.B. LePecq and C. Paoletti, *J. Mol. Biol.*, 1967, **27**, 87.
40 Q. Wang, Z.Y. Yang, G.F. Qi and D.D. Qin, *Eur. J. Med. Chem.*, 2009, **44**, 2425.
41 Z.A. Taha, A.M. Ajlouni, W.A. Momani and A.A. Al-Ghzawi, *Spectrochim. Acta A*, 2011, **81**, 570.
42 T.R. Li, Z.Y. Yang, B.D. Wang and D.D. Qin, *Eur. J. Med. Chem.*, 2008, **43**, 1688.